Journal of Manufacturing Processes 56 (2020) 540–549

Contents lists available at ScienceDirect

Journal of Manufacturing Processes

journal homepage: www.elsevier.com/locate/manpro

Application of linear friction welding for joining ultrafine grained aluminium

Marta Orłowska[a,*], Lech Olejnik[b], Davide Campanella[c], Gianluca Buffa[c], Łukasz Morawiński[b], Livan Fratini[c], Małgorzata Lewandowska[a]

[a] Faculty of Materials Science and Engineering, Warsaw University of Technology, Wołoska 141, 02-507 Warsaw, Poland
[b] Institute of Manufacturing Processes, Warsaw University of Technology, Narbutta 85, 02-524 Warsaw, Poland
[c] Department of Chemical, Management, Computer Science, Mechanical Engineering, University of Palermo, Viale delle Scienze, 90128 Palermo, Italy

ARTICLE INFO

Keywords:
Severe plastic deformation
Ultrafine grained microstructure
Aluminium
Linear friction welding

ABSTRACT

Ultrafine grained (UFG) materials are of great potential in industry due to their enhanced mechanical strength and other promising features, such as ability to superplastic deformation or excellent corrosion resistance. Nevertheless, one of the main limitations lies in their low thermal stability, which leads to excessive grain growth at elevated temperature. It influences mainly further processes performed at high temperature, such as joining. It causes detrimental problems during conventional fusion welding, as significant grain growth is observed and therefore the advantages as a result of small average grain size disappear. Therefore, the idea of applying solid state joining process seems to be suitable for UFG materials. Among the group of solid state welding processes there are methods based on friction. One of these methods, which is suitable for samples in the form of rectangular bars, is linear friction welding (LFW). Present study is the first comprehensive work describing the results of UFG aluminium welded using LFW method with additional emphasis put on a position of shear planes of welded samples. The results have shown, that UFG regime has not been preserved in a weld zone. Welding of UFG sample with an average grain size of 1 μm resulted in a grain growth in weld zone to 1.6 − 2 μm. Chosen parameters allowed to weld samples only locally, nevertheless, results from tensile tests performed on mini samples showed a great potential of the LFW method for joining UFG samples. The tensile strength of welds was in the range of 83–90 % of initial material.

1. Introduction

Bulk ultrafine grained (UFG) materials obtained by severe plastic deformation (SPD) processes [1] exhibit superior properties, such us enhanced hydrogen storage performance, superior thermoelectric properties, high magnetoresistance or enhanced electrical conductivity [2]. SPD methods allow to manufacture samples in different forms, such as rods or bars in equal channel angular pressing (ECAP) [3], plates by accumulative roll bonding (ARB) [4] or ECAP [5] or thin disc through high pressure torsion (HPT) [6]. Due to elevated number of structural defects, such as grain boundaries or dislocations, the enhancement in mechanical strength is observed. However, the main limitation of UFG materials is a lowered thermal stability, caused by the excess energy introduced during SPD processing. In case of aluminium and its alloys the thermal stability is preserved to the temperature of about 200 °C [7]. It limits the possibilities of applying welding techniques, which would preserve refined microstructure in the weld zone. Therefore, solid state welding methods are of great potential to apply to UFG materials. In paper [8] the welding abilities of UFG metals have been briefly analyzed. In present paper this topic will be described more in detail.

Friction welding (FW) methods are a group of techniques, which are based on a frictional heat between components, which occurs during the movement of them while being under pressure. Among FW techniques friction stir welding (FSW) [9], rotary friction welding (RFW) [10] and linear friction welding (LFW) [11] have to be mentioned. In work [12] the comparison between these three techniques was carried out. The common factor is the conditions of weld formation, which is conducted through plastic deformation at elevated temperature, caused by the heat generation due to the presence of friction. The temperature rises during the processes, however, it is below the melting point and depends on the process parameters and welded materials.

In case of UFG bulk materials obtained after SPD processing, papers devoted to welding are limited and are mainly focused on FSW of

* Corresponding author.
E-mail address: marta.orlowska.dokt@pw.edu.pl (M. Orłowska).

https://doi.org/10.1016/j.jmapro.2020.05.012
Received 18 February 2020; Received in revised form 10 May 2020; Accepted 11 May 2020

aluminium and its alloys [13–18] or copper [19]. It was shown that it is possible to obtain sound weld. Nevertheless, as a result of a temperature rise during the process, dynamic recrystallization occurs, which does not allow to preserve UFG structure in the stir zone. It was shown for UFG AA1050, that the grain growth from 600 nm to 4.3–4.56 μm has been achieved [13]. It caused a drop in microhardness and tensile strength of the weld, however, results were still higher than those obtained for fully annealed microstructure. In work [15] it has been shown that the initial grain size has an influence on a grain size in the weld zone. Despite the fact that the ultrafine range could not be maintained, the grain size increase was below 2 μm with a proper welding parameters. In the literature one can find also experiments with UFG structure steels, e.g. austenitic 304 L stainless steel, however refined microstructure was achieved through thermomechanical processing [20]. FSW process is of a high potential, however it's limitation is based on the sample's shape and it is limited to plates and sheets. For bulk rods or bars other FW techniques have to be used.

RFW process is an efficient method to weld samples with the round cross section. RFW method was used in work [21], where UFG structure 316 L stainless steel as a result of hydrostatic extrusion was welded. After plastic deformation, the microstructure consisted of strongly elongated bands in the extrusion direction with the thickness of ~100 nm. In the weld zone area the grain growth phenomena was observed, which partially eliminate the advantages of UFG structure, such as high microhardness. Moreover, authors observed that despite the high temperature close to the friction welding line, the combined recrystallization effect with the grain refinement on the friction surface results in a limitation of recrystallization. It was proved by the local increase of hardness.

In case of LFW process, samples with rectangular cross section can be welded together. The main idea of LFW process is to weld samples in a solid state under the pressure and with applying reciprocating movement. LFW consists of four stages [11]. In initial phase two samples are in contact under pressure. In this phase a heat is generated from solid friction and in case of its insufficient amount, the softening of the materials may be insufficient which can result that the next phase will not take place. The second phase is called the transition phase. In this phase contact area between welded elements is 100 %. Plastic deformation due to softening of samples starts to occur. Third, equilibrium phase initiates when the softened materials starts to extrude under the applied pressure. In the last phase, called deceleration phase, the reciprocating motion is inhibited. Additional axial force can be used in order to consolidate the weld.

LFW results in a formation of the characteristics zones on the weld's cross section. The zone, which is located in the place of the central weld line is called weld zone (WZ), where the microstructure is significantly different from the initial, base material. This is due to the phenomenon of recrystallization, which is caused by high temperature and large deformation occurring in this region of the weld. The second region is a thermomechanically affected zone (TMAZ). In this zone there are also changes in the microstructure, however, due to smaller deformations and lower temperature, which is associated with a greater distance from the central weld line, the changes are not as significant as in WZ. The third region is the heat affected zone (HAZ). In this part of the weld there are no more plastic deformations, but only the effect of temperature can be seen, which can cause changes in the microstructure. HAZ and TMAZ are called transition zone between base material and weld zone. The outer zone of the weld is a base material (BM). It is located at a distance from the central weld line, where it is not affected by temperature or plastic deformation. The size of the individual zones listed above depends on the LFW process parameters and welded material.

Increasing the amplitude and the frequency of oscillations a decrease in size of the HAZ zone can be obtained, with only little effect on WZ and TMAZ. The increase in amplitude and frequency causes faster heating and plasticizing of the material in the WZ, and thus reduces the friction stage time, so that the other zones (located further from the weld center) do not reach high temperature. The increase in the strength during the process reduces the size of WZ, TMAZ and HAZ. This effect can be explained by faster element shortening and heat dissipation from the weld area. The heat is removed from the weld area along with the effluent, reducing the temperature of the element in the weld area. In addition, the reduced friction phase time means that the heat released can only affect the rest of the material for a short time. The greater the force, the lower the temperature will be obtained in the weld area. Low temperature, as well as high pressure, limits the width of the WZ, TMAZ and HAZ. Not only the set parameters of the movement and the set values of the process forces, but also the dimensions of the connected elements matter. The smaller the dimension of the elements in the direction of oscillation, the smaller the WZ and TMAZ areas.

LFW, similarly to other solid state joining techniques, which are based on friction, has many advantages in comparison to conventional fusion welding techniques. These advantages includes but are not limited to lack of defects connected with solidification, such as porosity or hot cracking, or possible increase in mechanical properties in WZ due to recrystallization. Moreover, the process does not require additional consumables, its parameters are easy to control, therefore, there is a high reproducibility. Both similar and dissimilar welds can be manufactured. Among the disadvantages the major ones are as follows - limitation in shape of welded elements, the necessary requirements of plastically deformable component and flash, which occurs during the welding and which has to be removed.

LFW process was mainly investigated for Ti alloys, e.g. [22–26], however works concerning aluminium alloys, where both similar and dissimilar welds are produced were also investigated [27–30]. Results presented in this paper are one of the first, which describe the results obtained for UFG aluminium welded using LFW process. The aim of the study is to investigate the potential of joining UFG aluminium with this welding technique. UFG structure was obtained as a result of ECAP-based deformation process. Due to the rectangular shape of welded samples in LFW method, the influence of shearing planes has been also considered.

2. Methodology

Aluminium 1070 with 99.70 wt.% of purity was subjected to multi-turn ECAP (mtECAP) process, according to the procedure described in [31]. Chosen deformation route is presented in Fig. 1. During single pass, because of the shearing reverse, the second turn of the batch is equivalent to a 180° rotation, which is assigned to route C in ECAP notation [32]. Samples were rotated between each pass by 90°, which corresponds to route B_C. Therefore, the applied deformation route in the used in present study S-shaped channel was assumed as route C + B_C. Four passes resulted in equivalent strain equaled 9.2.

For LFW experiments samples were cut along the long axis of the deformed samples after mtECAP. The scheme and of the cut-out samples together with a scheme of weld's dimensions are shown in Fig. 2. The configuration of welded samples in accordance to marked in red shearing plane is presented in Fig. 3. Beside different shearing plane position, welds were also welded under different parameters. Oscillation direction was perpendicular to the plane with marked shearing planes seen in Fig. 3. Due to the importance of shearing planes, microstructure observations were conducted on planes presented in this figure, which is plane Y (flow plane) according to ECAP notation.

For the general view of the welds metallographics samples were used, which were previously grinded on a grit paper and polished using diamond suspensions. Observations were conducted on a light microscope (LM) Nikon Niphot. The detailed microstructure investigation was performed on a scanning electron microscope (SEM) Hitachi Su-70 equipped with the electron backscatter diffraction (EBSD) detector. Samples for observations on SEM were ground to the thickness of 150

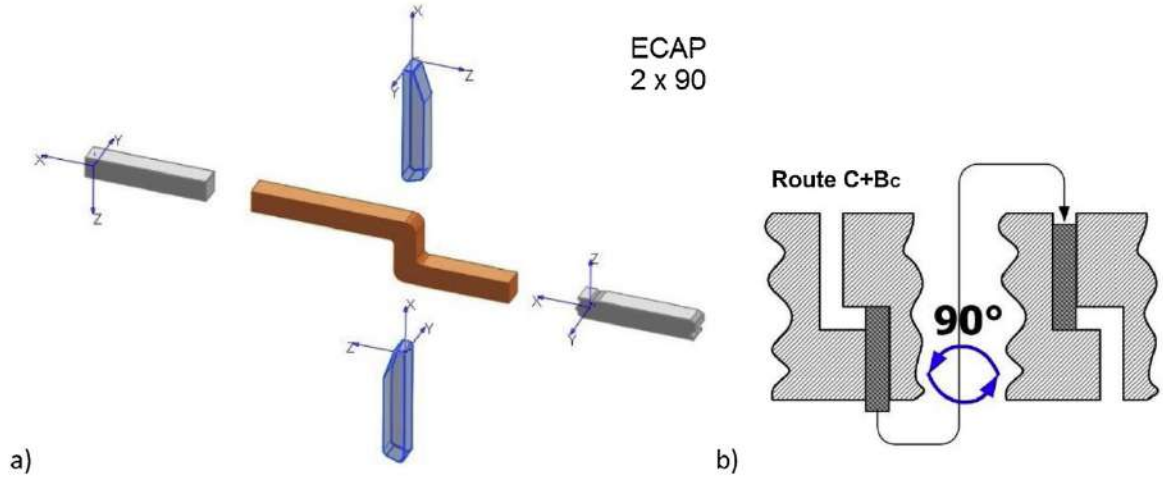

Fig. 1. Schematic illustration of a) mtECAP process with b) chosen deformation route (C + B_C).

μm and then electropolished on a Struers Tenupol-5 system operating at a voltage of 35 V at temperature of 278 K. The solution containing ethanol, perchloric acid, butyl glycol and distilled water was used. The final step was ion polishing on IM4000 ion polisher. The quantitative data, such as average grain/subgrain size and the fraction of low (LAGBs, $3° \leq \Phi \leq 15°$) and high angle grain boundaries (HAGBs, $\Phi > 15°$) were determined based on EBSD measurements.

To characterize mechanical properties, both tensile tests and microhardness measurements were carried out. In the first case, due to the dimensions of the welds, flat mini samples were used. The scheme of the samples is presented in Fig. 4. Digital Image Correlation (DIC) was used for accurate strain determination. For each weld three specimens were investigated. Tensile tests were also conducted for initial, UFG sample. Tests were performed at room temperature on a MTS Q Test/10 machine at a strain rate 10^{-3} s^{-1}. Also, macro images of samples after the tensile tests are presented. Microhardness measurements were carried out under a load of 200 g for 15 s. For each weld, a profile of microhardness was conducted with a step size 0.25 mm. Measurements were performed across the centre of a weld cross section.

3. Results and discussion

3.1. Microstructure evolution

The microstructure of AA1070 after mtECAP together with orientation map (OIM) is presented in Fig. 5. Plastic deformation resulted in a microstructure with the average grain size of 1.03 μm. Fraction of HAGBs is 62.2 %. Grains are elongated in accordance to the shearing direction with a variety of misorientations. Applied deformation route (C + B_C) determines the arrangement of the shear planes, which results in microstructure elements. Route B_C is the most effective in case of formation of equiaxial grains with a high fraction of HAGBs due to a large angular range of shearing planes [33]. Route C results in more elongated grains. Rotation by 180° reverses the shear strain every alternate cycle and the redundant strain causes cell blocks within the grains to rotate back to their original orientations. This prevents the formation of considerable numbers of new HAGBs [34]. Obtained microstructure is a result of the combination of these two routes. The average grain size is also influenced by the purity level.

Observed in SEM micrographs white particles are the primary intermetallic particles, frequently observed in commercially pure aluminium. They are rich in Fe and Si. It was already shown that both, plastic deformation and friction based welding process can results in their fragmentation, however such particles mainly influence corrosion resistance [35] and they influence a microstructure only in their closest vicinity. During deformation higher dislocation density and lattice misorientations may occur in the surrounding of such particles [36]. In present study their influence on microstructure will not be discussed.

The cross sections of the welds are presented in Fig. 6. In all cases, a sound weld has not been completely achieved on the whole contact line. Evidence of presence of characteristic flash for LFW process [10] cannot be seen due to the observation of perpendicular plane to the oscillation direction. Welds A and B seem to be the least properly welded. There are defects such as cracks on the whole interface between welded elements. Process parameters in each case are not optimal. From experimental and simulation results presented in work [37]

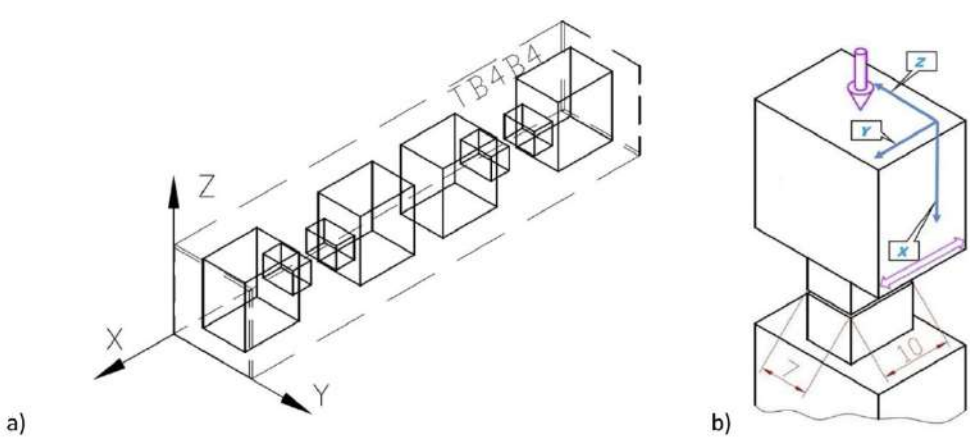

Fig. 2. The scheme of a) samples cut from the billet and b) weld dimensions.

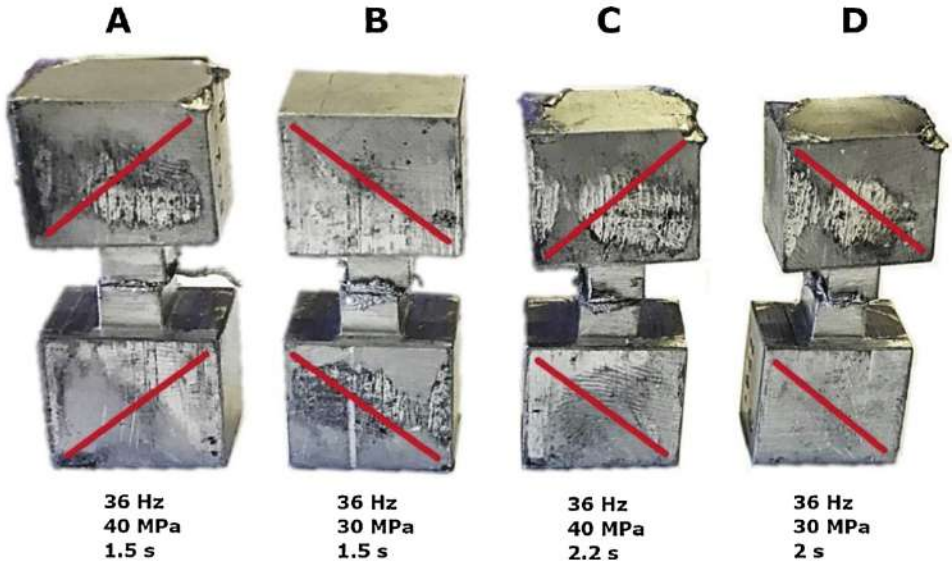

Fig. 3. Weld's configuration with marked in red shearing plane position, together with LFW process parameters.

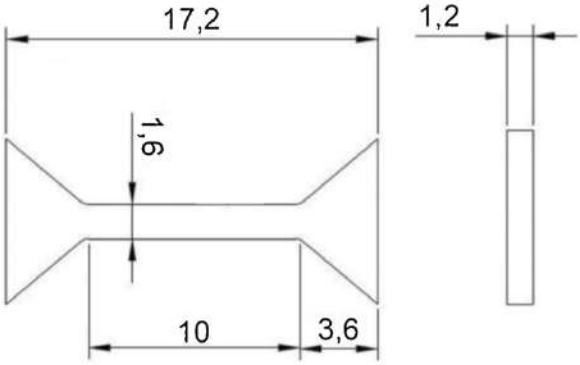

Fig. 4. Scheme of used flat mini-samples for tensile tests.

it was revealed, that two workpieces alignment results in a periodic extrusion and backflow of materials. When process achieves the quasi-steady state stage, compressive deformation plays a predominant role in the area close to the interface. Shear deformation occurs in a periodic manner in the periphery area of the interface when the oscillatory velocity becomes zero. Plastic deformation behavior is strongly dependent to LFW process parameters. The velocity of material flow at the interface of welded samples increases with the increase in oscillatory parameters, which is caused by the higher interfacial temperature. From the other side, the material flow is insufficient when the temperature rise is too low, which can be obtained with increasing friction pressure.

It was shown in work [27], that LFW of aluminium and its alloys is challenging due to their high thermal conductivity which impedes the heat concentration at the weld interface, making sound welding difficult to achieve. For such materials the parameters, e.g. frequency and pressure with respect to the material flow stress at the processing temperatures, to obtain sound weld are limited. Sufficient heat flux density is required because the heat generated at the interface diffuses to the base metal. Therefore, the friction pressure has to be sufficient to achieve necessary heat input. However, from the other side, too high pressure may lead to excessive deformation due to low mechanical properties of aluminium and its alloys. To overcome such difficulties with welding of high-thermal-conductivity materials such as aluminium alloys, another approach in welding was proposed, namely high-frequency LFW (HFLFW) [30]. Also, larger amplitude can be applied, however it may result in a wider edge zone and flash.

In addition, in case of UFG materials after ECAP-based processes another parameter may play a role in terms of sound weld formation. For such materials the behaviour during compressive depends on the shearing plane position, which was previously obtained in the last pass of ECAP process [8]. Improper shear planes position results in a sliding in the early stage of free upsetting process, which causes longitudinal axis deviations. Therefore, similarly in present study the position of shear planes may influence the proper weld formation. Nevertheless, based on macroscopic images of cross section of welds it can be stated, that more influencing factor is welding time. Between welds B and D, the difference lies only in extended time from 1.5 s to 2 s. The most promising results in terms of weld formation was obtained for welds C and D, which differed in a shear planes position. In case of weld C, where shearing planes were aligned in a different manner than in other welds, the geometry is preserved and welded samples are lined up

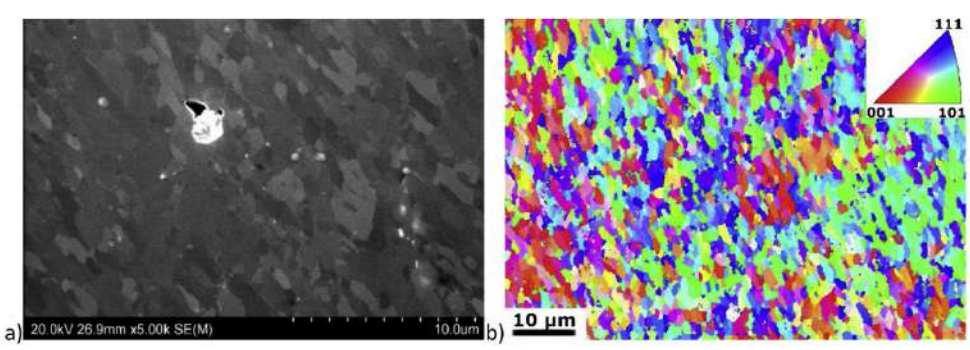

Fig. 5. a) SEM micrograph and b) OIM of ultrafine grained AA1070.

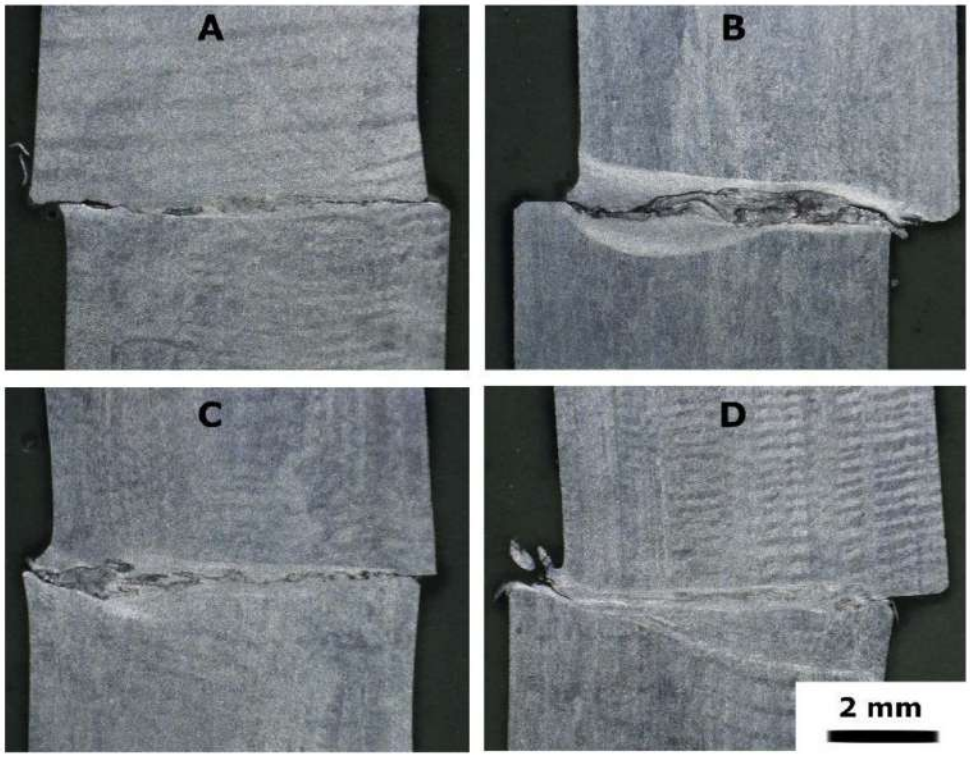

Fig. 6. Macrographs of the cross section of the welds.

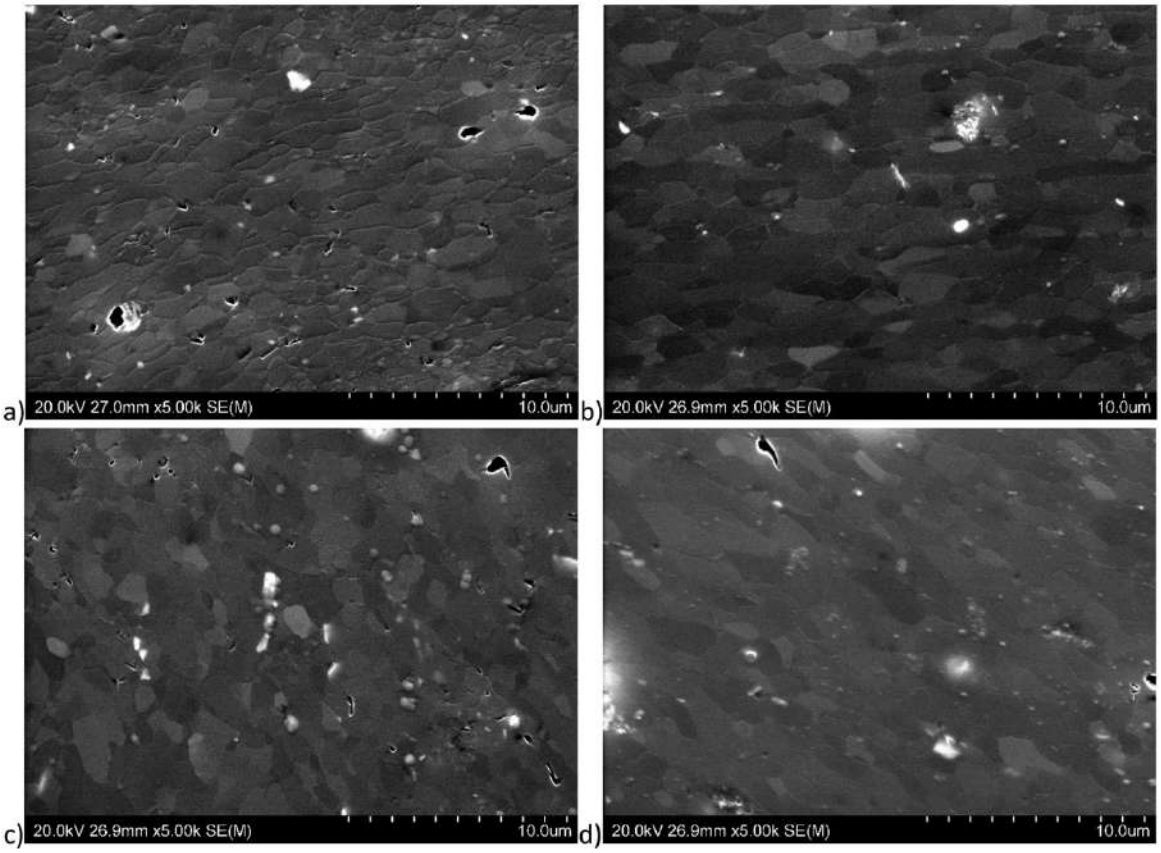

Fig. 7. SEM micrograph of welds a) A, b) B, c) C and d) D.

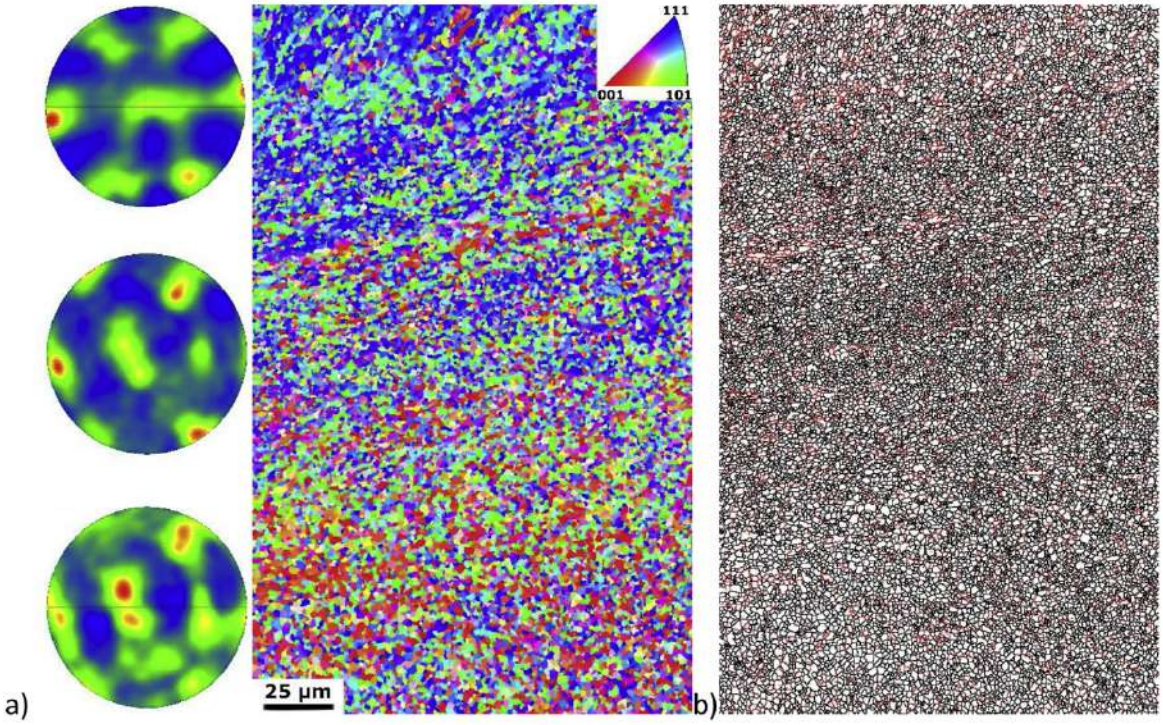

Fig. 8. a) OIM together with {111} pole figures and b) corresponding grain boundaries distribution (LAGBs – marked in red, HAGBs – marked in black) of weld D from the BM (top) to the WZ (bottom).

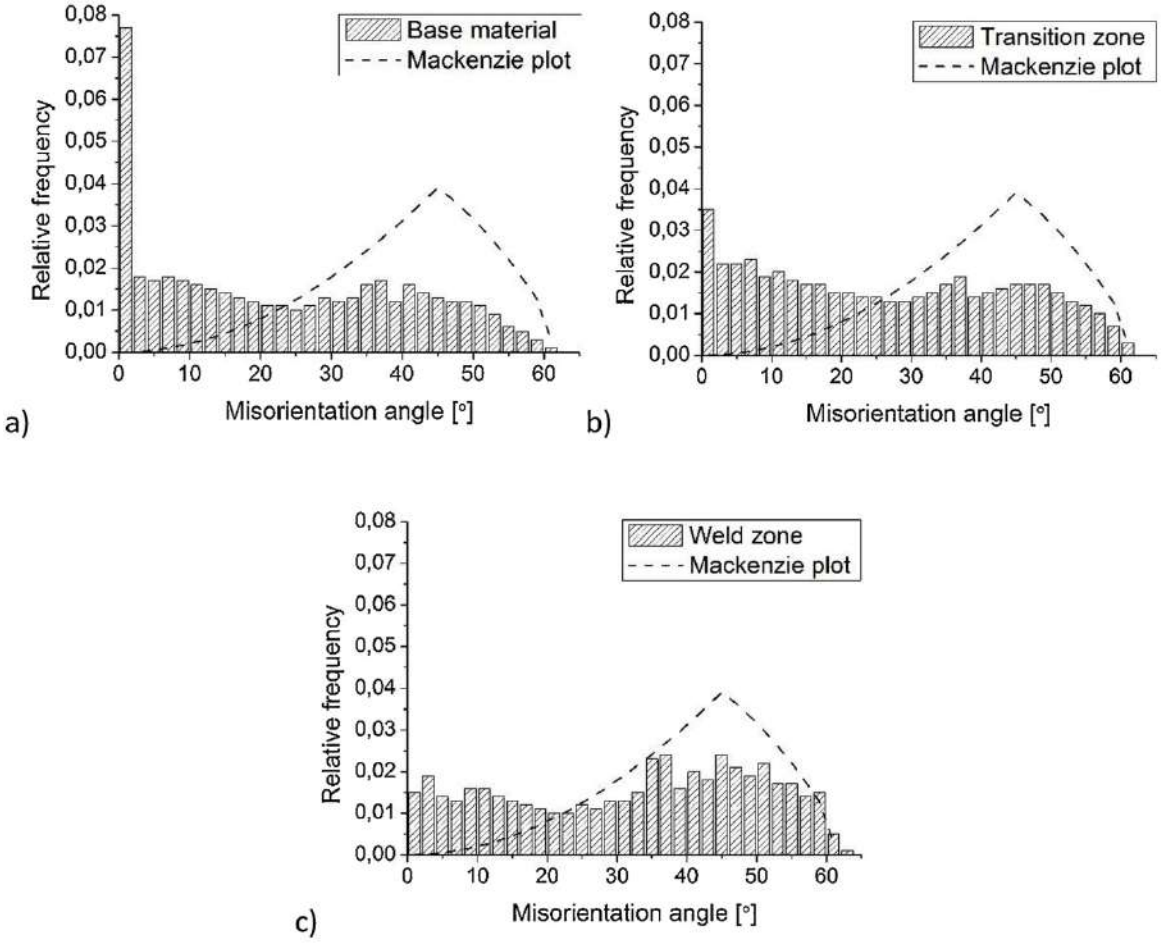

Fig. 9. Misorientation angle distributions of a) base material, b) transition zone and c) weld zone.

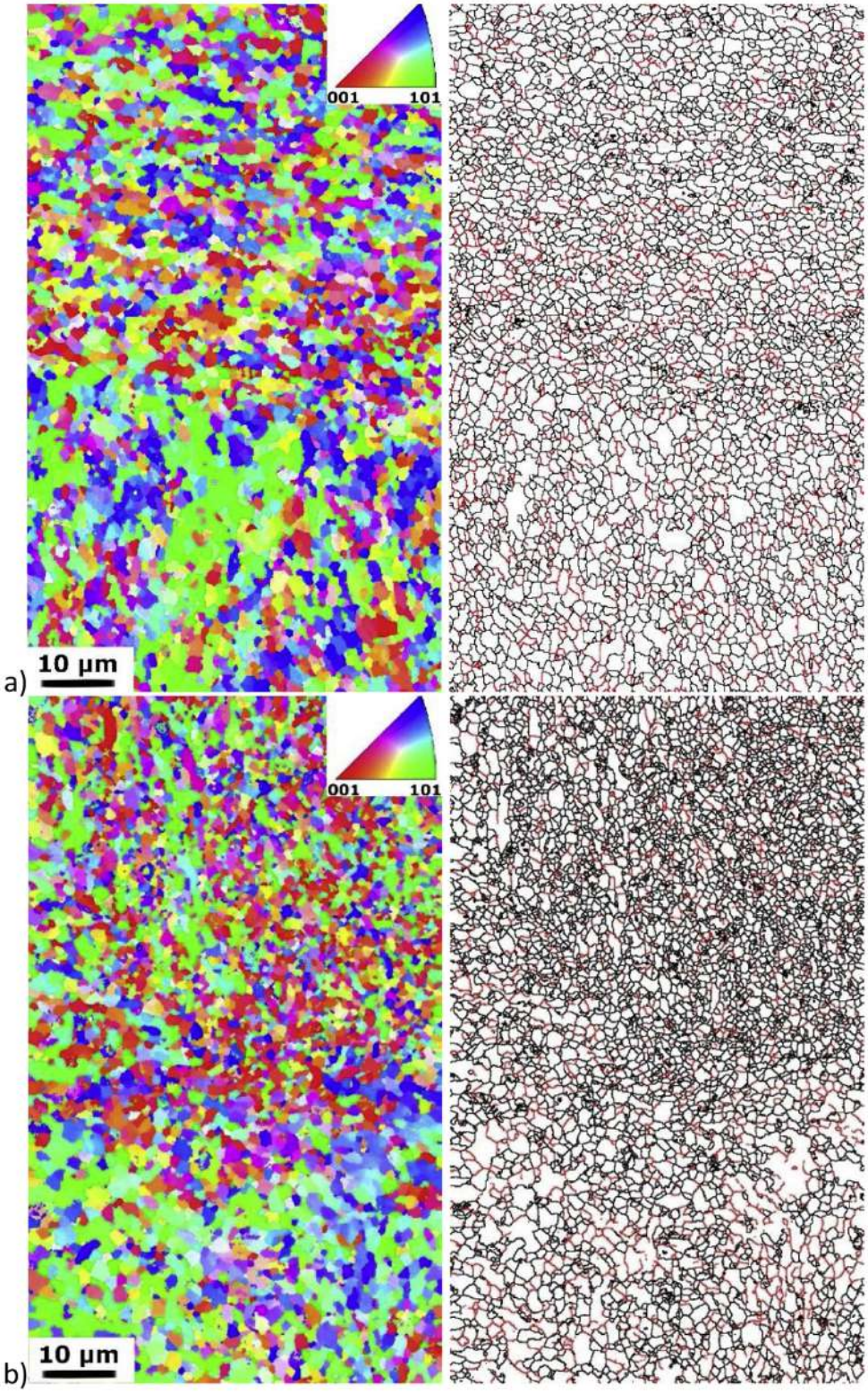

Fig. 10. OIMs grain boundaries distribution (LAGBs marked in red, HAGBs marked in black) of the cross-sections of the welds a) C and b) D from the transition zone (top) to the WZ (bottom).

without inclination seen in welds B and D. Nonetheless, first further experiments with LFW process parameters should be taken into consideration in order to obtain a sound weld. Further, the investigation of the influence of shear plane position should be examined.

The microstructure of WZ in each particular weld is presented in Fig. 7. The presented micrographs are from areas which were properly welded in each case. The grain growth is observed to the value of 1.6 – 2 µm. The differences between particular welds are negligible and they are within the error limits. The biggest grains achieved the size up to 5 µm. The fraction of HAGBs increased to the value of 68–78 %.The highest fraction of HAGBs was achieved for WZ of weld D. The size and distribution of intermetallic particles have not changed. It has to be

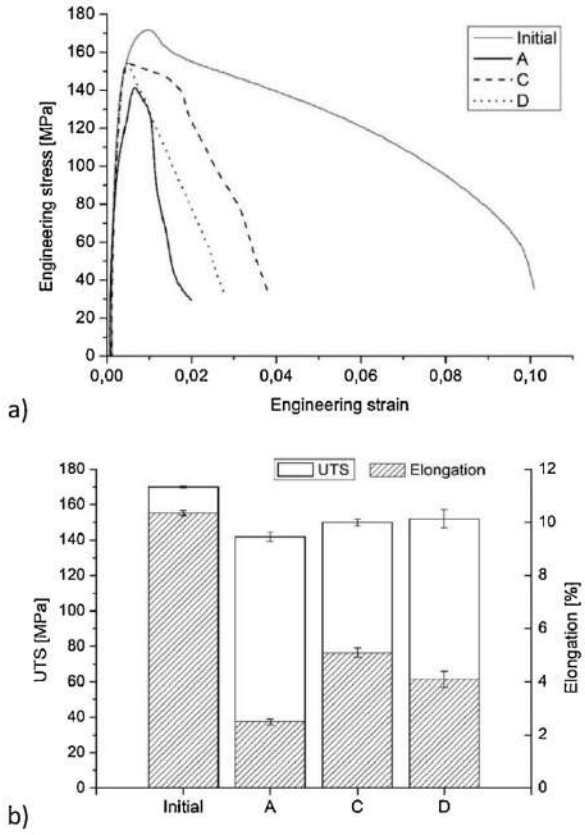

Fig. 11. a) Representative stress-strain curves of welds and base material and b) diagram of average values of UTS and elongation.

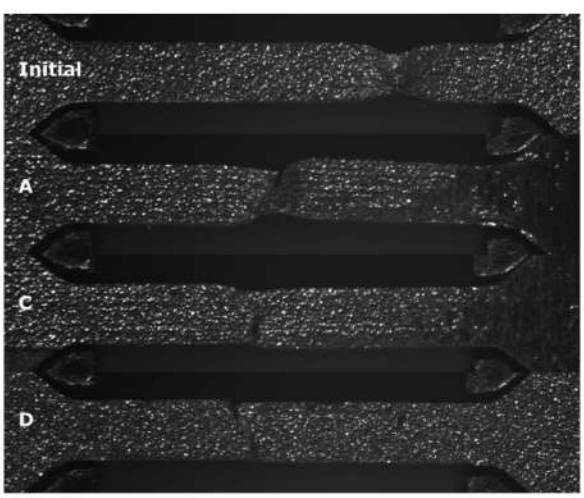

Fig. 12. Macro images of samples after tensile tests for initial material and welds.

emphasised that microstructure varies across the welds. Nevertheless, the increase in grain size is small in comparison to the results obtained for the commercially pure aluminium. For UFG AA1050 after FSW in the stir zone the grain growth from 600 nm to about 4.5 μm was obtained [13]. Smaller grain size was achieved in [15], where after ARB processing UFG AA1050 in stir zone after FSW the average grain size, depending on the process parameters, estimated 1.3–3.2 μm. In review of FSW/FSP processes [9] it was shown, that for coarse grained base materials, the recrystallization process in a weld zone can result in a wide range of grain size (1 − 20 μm), however, in order to achieve a size below 1 μm a special cooling has to be applied, e.g. liquid nitrogen.

In case of proper weld formation the microstructure in WZ is a result of dynamic recrystallization, which causes a formation of few micron sized equiaxial grains. When UFG material is welded, which is additionally thermally unstable, grain size in weld zone but also in transition zone is bigger than in base material. In present study process parameters allowed for small grain growth as compared to the base material. Even with improper weld formation, in each case the grain growth is similar in observed areas.

OIM together with a corresponding grain boundaries distribution of the cross section of the weld D are presented in Fig. 8. As can be seen, the changes in grain boundaries distribution and grain size are not significant at the present magnification. One can distinguish elevated density of boundaries in the TMAZ zone. More visible changes are observed in grains orientation shown in OIM. Attached pole figures {111} show that base material reveals characteristic for material after ECAP the shear texture. Texture consists of A and B fibres components, mainly of $A/\overline{A}$ $\{111\} < 110 >$, $B/\overline{B}$ $\{112\} < 110 >$ and C $\{001\} < 110 >$ shear components in accordance with the notation introduced in [38]. With approaching to the weld zone the changes in grains orientation are visible. Shear texture is vanishing and grains orientation became to be more random with preserved B fibre components.

Misorientation angle distributions from three regions – BM, transition zone and WZ are presented in Fig. 9. For BM there is a high peak for the angle 3°, which is typical for material after SPD processing. The majority of angles are of high angle type (above 15°), however, their distribution differs from the Mackenzie plot, which represents a theoretical distribution of randomly oriented cubic polycrystals [39]. Deviations from the Mackenzie plot indicate the occurrence of texture, which was seen in PF of base material. In transition zone the amount of HAGBs increases. Similarly in WZ, where the fraction of HAGBs is close to 80 %. Nevertheless, the deviation from Mackenzie plot still can be observed, indicating the presence of texture. However, as was seen from PFs, grains orientations are much more diverse in comparison to BM.

OIM together with corresponding grain boundaries of the transition area and WZ of weld C and D are shown in Fig. 10. With higher magnification more distinct differences in grain size are noticeable. It can be seen that weld zone area is characterized by bigger grain size in comparison to areas located further to the weld zone. Diverse grain orientation may indicate that recrystallization occurred in this weld. Even with insufficient process parameters to obtain sound weld, plastic deformation together with a temperature rise during LFW caused recrystallization in the WZ of welds. Nevertheless, differences between these two welds, at least in illustrated areas are negligible and does not allow to indicate the influence of process parameters or shear plane position on weld's microstructure.

3.2. Mechanical properties

The representative stress-strain curves for each weld and initial material are presented in Fig. 11a. For weld B it was not possible to perform tensile tests due to the presence of cracks in samples for tensile test. For initial material the characteristic curve for UFG materials was achieved. The flow stress quickly achieves the maximum value and then decreases gradually [40]. It shows that necking occurs early and further deformation is accompanied by a deepening neck. As a result, both uniform and elongation to break are limited and equals 10.5 % and about 1%, respectively. UTS and YS equals 170 MPa and 156 MPa, respectively. Curves for welds reveal fast achieving of maximum flow stress, after which fracture of welds occurred. Gathered results of UTS and elongation to failure are presented in diagram in Fig. 11b. UTS results of welds are lower than for base material. The highest result of UTS was obtained for welds C and D and estimates about 150 − 152 MPa, however for weld D the results are more scattered. The lowest value of UTS was achieved for weld A and equals 142 MPa. For this weld the elongation to failure value is the lowest, while the highest for

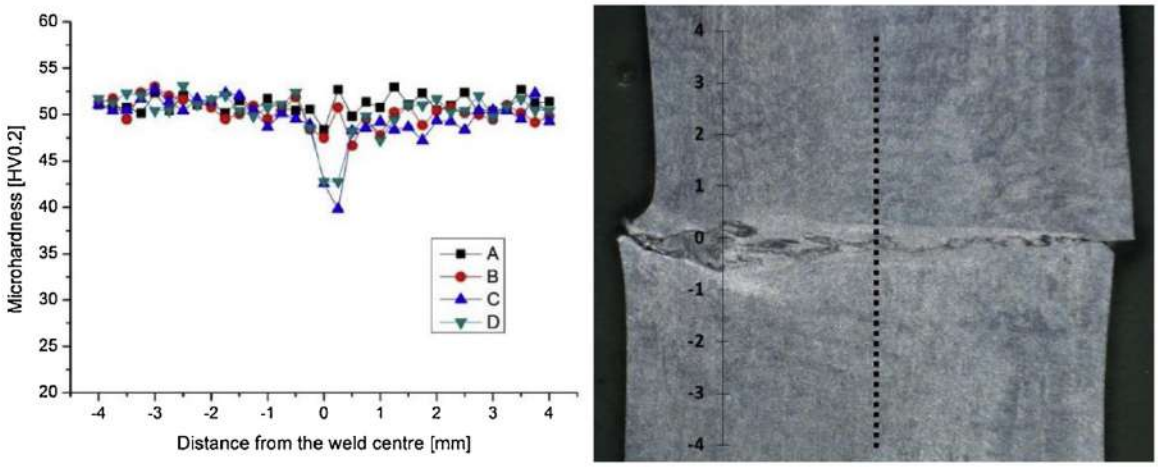

Fig. 13. Microhardness profiles of the cross-sections of the welds.

weld C. It indicates that the most promising results (UTS and elongation) are obtained for weld C. Error bars presented in the graphs indicate that initial sample is very homogenous, as differences between measured tensile samples are negligible. It is caused by the applied deformation route (C + B_C), which results in homogeneous UFG microstructure in the whole processed billet. In case of welds, bigger error bars means more significant variety in results. The biggest scatter was obtained for weld D. Such differences can be caused by more pronounced varieties of grain size at the weld's cross-sections.

For welds A and C the fracture occurred and the interface as can be seen in Fig. 12, indicating that sound weld has not completely occurred in these cases. For weld D, the fracture is shifted towards transition zone. Due to small dimensions of samples for tensile test it has to be emphasised that achieved results may not be fully reliable. High results of UTS could be occurred in only some areas of welds, as weld formation could be occurred only locally and not on the whole contact line between welded samples.

The microhardness profiles of the cross section of the welds together with the scheme of the points from which the measurements were taken are shown in Fig. 13. After mtECAP the microhardness value increased from ~25 HV0.2 to ~51 HV0.2. Therefore, grain refinement caused more than double increase in microhardness. As can be seen on microhardness profiles, changes in welds areas are observed. Nevertheless, for welds A and B, the decrease in microhardness is only about 3–4 HV0.2. It indicates that changes in microstructure are insignificant and proper weld formation has not been occurred. For the welds C and D the decrease in microhardness is more distinct and the drop is to the minimum value of 40–42 HV0.2. The drop is caused by the grain growth in this area. However, what has to be mentioned, the area affected by welding is very small in comparison to other works devoted to LFW, eg. for aluminium alloys [27][41].

In case of dissimilar welds of two aluminium alloys – 2011 and 6082, the maximum decrease to the value of 70 HV was obtained, with results for base materials equal 120 HV and 100 HV, respectively [28]. The differences in microhardness are as a result of differences in microstructure. Despite the distinct reduction in grain size, changes in second phase particles are responsible for that. The changes in microhardness in welds of aluminium alloys are connected, apart from process parameters, to material itself. As was shown in [41] for high-frequency LFW, both hardening and softening effects can be obtained, depending if aluminium alloy is work- or precipitation hardened. Similar results were achieved for different aluminium alloys in [30], where microhardness in work hardened AA 5052 increased for all tested process parameters, meanwhile for precipitation hardened AA 6063 only in the low heat input condition. However, what has to be mentioned, all mentioned results were obtained for base materials with coarse grained microstructure. There is a lack of works concerning LFW process on UFG materials. Nevertheless, in works describing welding of UFG aluminium using FSW method, microhardness in stir zone decreased due to recrystallization process which resulted in bigger grain size in the weld centre in comparison to BM, as can be seen in e.g. [15,17,42].

Welding of coarse grained materials using LFW method leads to the grain size reduction in WZ due to dynamic recrystallization process. In case of aluminium alloys it was shown e.g. in [28], where experiments with AA2011 and AA6082 were carried out. Depending on process parameters, it was possible to reduce average grain size up to few microns in the WZ. This result indicates that sufficient heat and deformation are produced to activate dynamic recrystallization, which is common in friction based processes. However, despite the reduction in grain size the microhardness in WZ decreased due to the heat effect and its influence on second phase particles, which next to grain boundaries are a material strengthening factor. Similar results were obtained in work [30], where two aluminium alloys 6063 and 5052 were welded using LFW. Since the 6063 Al alloy is a precipitation hardened, only this one was significantly affected by heat and the softening occurred in the WZ due to changes in precipitates condition. Despite the differences in microhardness, tensile tests of welds revealed that some of the welds pose the values of tensile tests as high as for the base material, even that non-destructive tests exhibited, the defects existed in the entire interface in the low-heat-input condition. Therefore, a strong weld would be achieved locally, resulting in excellent mechanical properties in the area welded soundly in a short friction time without heat effects.

Similar results were obtained in present study. Even macrographs of welds cross section (Fig. 6) show discontinuities, only for weld B tensile test were not possible to be performed. For other welds tensile tests reveal high tensile strength, in the range of 83–90 % of initial material. Nevertheless, it is assumed that samples are welded only locally. However, changes in grain size and orientation in welds C and D allow to draw a conclusion, that recrystallization occurred in the WZ. Results obtained for weld C may indicate, that shear planes location can have an effect on a weld formation. Nevertheless, process parameters are not optimal and further experiments have to be conducted, as LFW seems to be of a great potential to weld UFG materials. Moreover, influence of shearing plane position in relation to oscillation direction should be also taken into account, as it can determine the possibility to achieve a sound weld of UFG samples after ECAP-based processing.

4. Conclusions

In present work an attempt to weld ultrafine grained aluminium has been taken. Samples of AA1070 were processed using mtECAP and as a

result the microstructure consisting of ultrafine grains with the average size of about 1 μm and fraction of HAGBs equals 62 % has been obtained. Subsequently, samples were welded using LFW method. The grain growth in the weld zone was up to average value of 1.6 − 2 μm with a subsequent increase in fraction of HAGBs. Applied process parameters did not allow to obtain sound welds on the whole cross section, however, samples were welded locally. It was proved by tensile tests, which resulted in high values of UTS of welds. Also, in two welds a distinct drop in microhardness has been achieved, which may suggest that the recrystallization process occurred.

Achieved results show a great potential of LFW process in application for UFG materials, nevertheless, further experiments have to be performed. UFG metals produced by SPD processing require a different approach when selecting friction welding parameters in comparison to conventional, coarse grained materials. Also, taking into account the position of the shear plane when taking the material from the billet for welding - this requires a deeper and further examination.

Declaration of Competing Interest

The authors declare that there are no conflicts of interest.

Acknowledgements

This research was carried out within a Project financed by National Science Centre, Poland under the OPUS-14 fund (Contract no. UMO-2017/27/B/ST8/003491) and was additionally subsidized by Warsaw University of Technology.

References

[1] Valiev RZ, Estrin Y, Horita Z, Langdon TG, Zehetbauer MJ, Zhu Y. Producing bulk ultrafine-grained materials by severe plastic deformation. JOM 2006;58:33–9. https://doi.org/10.1007/s11837-016-1820-6.
[2] Valiev RZ, Estrin Y, Horita Z, Langdon TG, Zehetbauer MJ, Zhu YT, et al. Fundamentals of superior properties in bulk NanoSPD materials. Mater Res Lett 2016;4:1–21. https://doi.org/10.1080/21663831.2015.1060543.
[3] Valiev RZ, Langdon TG. Principles of equal-channel angular pressing as a processing tool for grain refinement. Prog Mater Sci 2006;51:881–981. https://doi.org/10.1016/j.pmatsci.2006.02.003.
[4] Saito Y, Utsunomiya H, Tsuji N, Sakai T. Novel ultra-high straining process for bulk materials—development of the accumulative roll-bonding (ARB) process. Acta Mater 1999;47:579–83. https://doi.org/10.1016/S1359-6454(98)00365-6.
[5] Kamachi M, Furukawa M, Horita Z, Langdon TG. Equal-channel angular pressing using plate samples. Mater Sci Eng. A 2003;361:258–66. https://doi.org/10.1016/S0921-5093(03)00522-7.
[6] Zhilyaev AP, Langdon TG. Using high-pressure torsion for metal processing: fundamentals and applications. Prog Mater Sci 2008;53:893–979. https://doi.org/10.1016/j.pmatsci.2008.03.002.
[7] Hasegawa H, Komura S, Utsunomiya A, Horita Z, Furukawa M, Nemoto M, et al. Thermal stability of ultrafine-grained aluminum in the presence of Mg and Zr additions. Mater Sci Eng A 1999;265:188–96. https://doi.org/10.1016/S0921-5093(98)01136-8.
[8] Morawiński Ł, Chmielewski T, Olejnik L, Buffa G, Campanella D, Fratini L. Welding abilities of UFG metals. AIP Conf Proc 2018:050012https://doi.org/10.1063/1.5034885.
[9] Mishra RS, Ma ZY. Friction stir welding and processing. Mater Sci Eng R Rep 2005;50:1–78. https://doi.org/10.1016/j.mser.2005.07.001.
[10] Li W, Vairis A, Preuss M, Ma T. Linear and rotary friction welding review. Int Mater Rev 2016;61:71–100. https://doi.org/10.1080/09506608.2015.1109214.
[11] Vairis A, Frost M. High frequency linear friction welding of a titanium alloy. Wear 1998;217:117–31.
[12] Vairis A, Papazafeiropoulos G, Tsainis A. A comparison between friction stir welding, linear friction welding and rotary friction welding. Adv Manuf 2016. https://doi.org/10.1007/s40436-016-0163-4.
[13] Lipińska M, Olejnik L, Pietras A, Rosochowski A, Bazarnik P, Goliński J, et al. Microstructure and mechanical properties of friction stir welded joints made from ultrafine grained aluminium 1050. Mater Des 2015;88:22–31. https://doi.org/10.1016/j.matdes.2015.08.129.
[14] Malopheyev S, Mironov S, Kulitskiy V, Kaibyshev R. Friction-stir welding of ultrafine grained sheets of Al-Mg-Sc-Zr alloy. Mater Sci Eng A 2015;624:132–9. https://doi.org/10.1016/j.msea.2014.11.079.
[15] Sun Y, Fujii H, Takada Y, Tsuji N, Nakata K, Nogi K. Effect of initial grain size on the joint properties of friction stir welded aluminum. Mater Sci Eng A 2009;527:317–21. https://doi.org/10.1016/j.msea.2009.07.071.
[16] Nikulin I, Malopheyev S, Kipelova A, Kaibyshev R. Effect of SPD and friction stir welding on microstructure and mechanical properties of Al-Cu-Mg-Ag sheets. Mater Lett 2012;66:311–3. https://doi.org/10.1016/j.matlet.2011.08.104.
[17] Topic I, Hoppel HW, Goken M. Friction stir welding of accumulative roll-bonded commercial-purity aluminium AA1050 and aluminium alloy AA6016. Mater Sci Eng A 2009;503:163–6. https://doi.org/10.1016/j.msea.2007.12.057.
[18] Khorrami MS, Kazeminezhad M, Kokabi AH. Microstructure evolutions after friction stir welding of severely deformed aluminum sheets. Mater Des 2012;40:364–72. https://doi.org/10.1016/j.matdes.2012.04.016.
[19] Barekatain H, Kazeminezhad M, Kokabi AH. Microstructure and mechanical properties in dissimilar butt friction stir welding of severely plastic deformed aluminum AA 1050 and commercially pure copper sheets. J Mater Sci Technol 2014;30:826–34. https://doi.org/10.1016/j.jmst.2013.11.007.
[20] Sabooni S, Karimzadeh F, Enayati MH, Ngan AHW. Friction-stir welding of ultrafine grained austenitic 304L stainless steel produced by martensitic thermomechanical processing. Mater Des 2015;76:130–40. https://doi.org/10.1016/j.matdes.2015.03.052.
[21] Skowornska B, Chmielewski T, Pachla W, Kulczyk M, Skiba J, Presz W. Friction weldability of UFG 316L stainless steel. Arch Metall Mater 2019;64:1051–8. https://doi.org/10.24425/amm.2019.129494.
[22] Vairis A, Frost M. On the extrusion stage of linear friction welding of Ti 6Al 4V 271. 1999. p. 477–84.
[23] Ma T, Chen T, Li W, Wang S, Yang S. Formation mechanism of linear friction welded Ti–6Al–4V alloy joint based on microstructure observation. Mater Charact 2010;62:130–5. https://doi.org/10.1016/j.matchar.2010.11.009.
[24] Boyat X, Ballat-durand D, Marteau J, Bouvier S, Favergeon J, Orekhov A, et al. Interfacial characteristics and cohesion mechanisms of linear friction welded dissimilar titanium alloys: Ti-5Al-2Sn-2Zr-4Mo-4Cr (Ti17) and Ti–6Al–2Sn–4Zr–2Mo (Ti6242). Mater Charact 2019;158:109942https://doi.org/10.1016/j.matchar.2019.109942.
[25] Karadge M, Preuss M, Lovell C, Withers PJ, Bray S. Texture development in Ti–6Al–4V linear friction welds. Mater Sci Eng A 2007;459:182–91. https://doi.org/10.1016/j.msea.2006.12.095.
[26] McAndrew AR, Colegrove PA, Bühr C, Flipo BCD, Vairis A. A literature review of Ti-6Al-4V linear friction welding. Prog Mater Sci 2018;92:225–57. https://doi.org/10.1016/j.pmatsci.2017.10.003.
[27] Fratini L, Buffa G, Cammalleri M, Campanella D. On the linear friction welding process of aluminum alloys: experimental insights through process monitoring. CIRP Ann Manuf Technol 2013;62:295–8. https://doi.org/10.1016/j.cirp.2013.03.056.
[28] Buffa G, Cammalleri M, Campanella D, La Commare U, Fratini L. Linear friction welding of dissimilar AA6082 and AA2011 aluminum alloys: microstructural characterization and design guidelines. Int J Mater Res 2017;10:307–15. https://doi.org/10.1007/s12289-015-1279-y.
[29] Buffa G, Cammalleri M, Campanella D, Fratini L. Shear coefficient determination in linear friction welding of aluminum alloys. Mater Des 2015;82:238–46. https://doi.org/10.1016/j.matdes.2015.05.070.
[30] Mogami H, Matsuda T, Sano T, Yoshida R, Hori H, Hirose A. High-frequency linear friction welding of aluminum alloys. Mater Des 2018;139:457–66. https://doi.org/10.1016/j.matdes.2017.11.043.
[31] Olejnik L, Rosochowski A. Scaled-up ECAP with enhanced productivity. Met Form 2008;2:439–46.
[32] Langdon TG, Furukawa M, Nemoto M, Horita Z. Using equal-channel angular pressing for refining grain size. JOM 2000;52:30–3. https://doi.org/10.1007/s11837-000-0128-7.
[33] Iwahashi Y, Horita Z, Nemoto M, Langdon TG. The process of grain refinement in equal-channel angular pressing. Acta Mater 1998;46:3317–31. https://doi.org/10.1016/S1359-6454(97)00494-1.
[34] Gholinia A, Prangnell PB, Markushev MV. Effect of strain path on the development of deformation structures in severely deformed aluminium alloys processed by ECAE. Acta Mater 2000;48:1115–30. https://doi.org/10.1016/S1359-6454(99)00388-2.
[35] Lipińska M, Ura-Bińczyk E, Olejnik L, Rosochowski A, Lewandowska M. Microstructure and corrosion behavior of the friction stir welded joints made from ultrafine grained aluminum. Adv Eng Mater 2017;19:1–10. https://doi.org/10.1002/adem.201600807.
[36] Humphreys FJ. The nucleation of recrystallization at second phase particles in deformed aluminium. Acta Metall 1977;25:1323–44. https://doi.org/10.1016/0001-6160(77)90109-2.
[37] Geng P, Qin G, Chen L, Zhou J, Zou Z. Simulation of plastic flow driven by periodically alternating pressure and related deformation mechanism in linear friction welding. Mater Des 2019;178:107863https://doi.org/10.1016/j.matdes.2019.107863.
[38] Toth LS, Neale KW, Jonas JJ. Stress response and persistence characteristics of the ideal orientations of shear textures. Acta Metall 1989;37:2197–210.
[39] Mackenzie JK. Second paper on statistics associated with random disorientation of cubes. Biometrika Trust 1958;45:229–40.
[40] Horita Z, Fujinami T, Langdon TG. The potential for scaling ECAP: effect of sample size on grain refinement and mechanical properties. Mater Sci Eng A 2001;318:34–41. https://doi.org/10.1016/S0921-5093(01)01339-9.
[41] Lis A, Mogami H, Matsuda T, Sano T, Yoshida R, Hori H. Hardening and softening effects in aluminium alloys during high-frequency linear friction welding. J Mater Process Tech 2018;255:547–58. https://doi.org/10.1016/j.jmatprotec.2018.01.002.
[42] Khorrami MS, Kazeminezhad M, Kokabi AH. Mechanical properties of severely plastic deformed aluminum sheets joined by friction stir welding. Mater Sci Eng A 2012;543:243–8. https://doi.org/10.1016/j.msea.2012.02.082.